Published in final edited form as:
Exp Biol Med (Maywood). 2011 September 1; 236(9): 1051–1063. doi:10.1258/ebm.2011.010400.

Dietary Wolfberry Ameliorates Retinal Structure Abnormalities in db/db Mice at the Early Stage of Diabetes

Ling Tang[‡,1], **Yunong Zhang**[‡,1], **Yu Jiang**[‡,1], **Lloyd Willard**[2], **Edlin Ortiz**[1], **Logan Wark**[1], **Denis Medeiros**[1], and **Dingbo Lin**[1,*]

[1]Department of Human Nutrition, Kansas State University, Manhattan, KS 66506

[2]Department of Diagnostic Medicine/Pathobiology, Kansas State University, Manhattan, KS 66506

Abstract

Hyperglycemia-linked oxidative stress and/or consequent endoplasmic reticulum stress are the causative factors of pathogenesis of diabetic retinopathy. Dietary bioactive components which mitigate oxidative stress may serve as potential chemopreventative agents to prevent or slow down the disease progression. Wolfberry is a traditional Asian fruit consumed for years to prevent aging eye diseases in Asian countries. Here we report that dietary wolfberry ameliorated mouse retinal abnormality at the early stage of type 2 diabetes in db/db mice. Male mice at 6 weeks of age were fed the control diet with or without 1 % (kCal) wolfberry for 8 weeks. Dietary wolfberry restored the thickness of the whole retina, in particular the inner nuclear layer and photoreceptor layer, and the integrity of retinal pigment epithelia (RPE), and the ganglion cell number in db/db mice. Western blotting of whole retinal cell lysates revealed that addition of wolfberry lowered expression of endoplasmic reticulum (ER) stress biomarkers BiP, PERK, ATF6, and caspase-12; and restored AMPK, thioredoxin, Mn SOD, and FOXO3α activities. To determine if our observations were due to the high contents of zeaxanthin and lutein in wolfberry additional studies using these carotenoids were conducted. Using the human adult diploid RPE cell line ARPE-19 we demonstrated that both zeaxanthin and lutein could mimic wolfberry preventive effect on activation of AMPK, thioredoxin, Mn SOD, FOXO3α activities, normalize cellular reactive oxygen species, and attenuate ER stress in ARPE-19 cells exposed to a high glucose challenge. The zeaxanthin preventive effect was abolished by siRNA knockdown of AMPKα. These results suggested that AMPK activation appeared to play a key role in upregulated expression of thioredoxin and Mn SOD, and mitigation of cellular oxidative stress and/or ER stress by wolfberry and zeaxanthin and/or lutein. Taken together, dietary wolfberry on retinal protection in diabetic mice is, at least partially, due to zeaxanthin and/or lutein.

Keywords

AMPK; Diabetic retinopathy; ER stress; reactive oxygen species; wolfberry; zeaxanthin

Introduction

Diabetic retinopathy is a retinal damage caused by complications of diabetic mellitus. It is the leading cause of vision impairment and blindness in working age adults. Unfortunately,

[*]**Corresponding author: Dingbo Lin, PhD,** Department of Human Nutrition, Kansas State University, 212 Justin Hall, Manhattan, KS 66506, Phone: 785-532-2184, Fax: 785-532-3132, dingbo@ksu.edu.
[‡]equal contribution

Conflict of interest: No

no permanent cure is currently available. It is well accepted that hyperglycemia is a major causative factor of the progression of the disease (1,2). At the early stage of diabetes retinal blood microvessels are still intact and no observable blood leakage occurs. However, hyperglycemia-induced cellular oxidative stress would alter cellular energy homeostasis, mitochondria biogenesis, and metabolic activity, for instance down-regulation of AMP-activated protein kinase (AMPK) (3-5).

AMPK is a trimeric serine/threonine kinase and functions as a cellular energy sensor to maintain cellular energy homeostasis. AMPK consists of a catalytic α subunit and non-catalytic β and γ subunits. The α subunit has a NH_2-terminal catalytic kinase domain and a COOH-terminal regulatory domain where the β and γ subunits bind. Phosphorylation of the AMPK α subunit (AMPK α) on Thr172 causes activation of AMPK (3). AMPK has been proposed to mediate hyperglycemia-induced reactive oxygen species (ROS) production in mitochondria (5). Prolonged diabetic inhibition of AMPK causes mitochondria dysfunction and disruption of cellular reactive oxygen species (ROS) homeostasis (5, 6). Thus, AMPK signaling could be a novel target for diabetic therapy (7).

Hyperglycemia-linked oxidative stress disrupts protein synthesis and protein folding in the endoplasmic reticulum (ER) among diabetic patients (8,9). Studies have suggested that protein unfolding and/or misfolding in the ER would eventually lead to ER stress, and subsequent cell apoptosis (10,11). Three signaling pathways are involved in ER stress, which include three ER stress transducer proteins inositol-requiring protein-1 (IRE1), activating transcription factor 6 (ATF6), and protein kinase RNA-like ER kinase (PERK), and an ER stress sensor protein binding immunoglobulin protein (BiP) (10, 12-14). In unstressed cells, BiP binds to and inactivates IRE1, ATF6, and/or PERK. When the ER stress occurs, protein expression levels of BiP, IRE1, ATF6 and PERK are elevated. BiP dissociates from all three transducers, which triggers activation of those three transducer-mediated signaling pathways, and subsequently leads to induction of C/EBP homologous protein transcription factor, and activation of c-Jun NH2-terminal kinase and caspase, which eventually results in apoptosis in diabetes (12-14). Thus, ER stress has been considered as a major driven force to cellular oxidative damage in the diabetic retina (13).

Wolfberry (*Lycium barbarum* L., Chinese name Goji berry) is a fruit which has been consumed for hundreds of years in China and Eastern Asia to prevent eye diseases. It was exported to Western countries in the last century. Fresh wolfberry fruits are bright orange-red, oblong shaped. They can be purchased fresh or as a dried fruit, drink, and/or a wine. Wolfberry contains large amounts of lutein and zeaxanthin in ester forms, which are neuroprotective in the progression of macular degeneration (14,15). Zeaxanthin and lutein are dominantly enriched in the RPE and other retinal layers, particularly within the central macula (14). In addition, wolfberry contains significant amount of polysaccharides and phenolics (14,16,17). Small molecules such as betaine, cerebroside, various vitamins, and zinc are observed in wolfberry as well (14,17,18). According to traditional Chinese medicine literature, wolfberry can nourish liver and kidney, help re-balance of the “Yin” and “Yan”. (i.e., energy homeostasis), boost immune system, and improve vision. However, the molecular mechanisms of how the bioactive constituents of wolfberry exert their influence on vision are not well understood.

This study sought to determine the nature of the preventive effect of dietary wolfberry and/or its bioactive components zeaxanthin and lutein on diabetic retinopathy using models of the db/db leptin receptor deficient type 2 diabetic mouse in vivo and the human RPE cell culture in vitro. The results suggested that wolfberry, zeaxanthin and/or lutein ameliorated retinal damage and this could be due to the restoration of AMPK and its downstream target proteins involving attenuation of ER stress and/or oxidative stress in the diabetic retina and

in the human RPE cell exposed to a high glucose challenge. These finding could lead to the development of complementary dietary regimens for prevention or delay of the onset of retinopathy at the early stage of type 2 diabetes.

Materials and Methods

Animal, wolfberry, and design

Six-week-old male wild type (C57BLKS/J, abbrev. WT) and type 2 diabetic (BKS.C g-m+/+ *Lepr*^{db}/J, abbrev. db/db) mice were purchased from Jackson Laboratory (Bar Harbor, Massachusetts, USA). Forty two db/db and 42 WT mice were equally divided into two treatment groups, respectively. One group of mice were fed a regular control diet (CD, n=21) and the other group were fed a control diet with addition of 1% (kCal) wolfberry (Wolfberry Diet, WD, n=21). The diets were formulated and purchased from the Research Diets Inc (Table 1) (New Brunswick, NJ, USA).

Wolfberry used in this project was from the same batch of the “Zhongning” wolfberry which was purchased from Zhongning, Ningxia, China, through a local grocery store. Macronutrient contents of wolfberry fruits were analyzed in the Analytical Service Laboratory at Kansas State University (202 Weber Hall, Manhattan, KS, USA). About 68.2 % of the mass of dried wolfberry fruits was carbohydrate, 11.8 % was protein, and 8.6 % was fat, giving a total caloric value in a 100 g serving of about 397 kCal (estimated calories=protein × 4 +carbohydrate × 4 +fat × 9). Thus, Wolfberry diet contained 10.7 g wolfberry fruits in the control diet per 4057 kCal (10.7 g/ 4057 kCal) (Table 1). Animals were fed their respective diets for 8 weeks. Food consumption and blood glucose were tracked on a weekly basis. All experiments conformed to the Association for Research in Vision and Ophthalmology Statement for Use of Animals in Ophthalmic and Vision Research and were performed under an institutionally approved animal protocol.

Mice were group housed (3/cage) in a controlled environment with a 12-h light/dark cycle at a constant room temperature. All animals had free access to water and food throughout the study. After 8 weeks, animals were sacrificed by CO_2 according to the approved protocols. Blood samples were collected for plasma insulin measurement. Note, in our preliminary study we observed that CO_2 euthanization did not cause any significant change of insulin levels in both animal groups WT and db/db, compared to that of cervical dislocation. Heart, kidney, liver, and right eyes were removed, weighed, and placed in liquid nitrogen immediately, then stored at −80°C until processed for protein extraction. The left eyes of mice were removed and fixed for light microscopy.

Fasting blood glucose test

A drop of blood (~ 5 μL) was collected from 6 h fasting mice by a tail snip. Blood glucose was tested by the Precision Xtra® blood glucose monitoring system (Alameda, CA, USA), according to the manufacturer’s instruction.

Plasma insulin measurement

Fasting (6 h) blood samples were collected into PST™ tubes with polymer gel and lithium heparin (BD, Franklin Lakes, NJ, USA). Plasma was separated by centrifugation. Plasma insulin level was determined using the ultra sensitive mouse insulin ELISA kit (Crystal Chem, Downers Grove, IL, USA), following the manufacturer’s instruction.

Human RPE cell culture and a high glucose challenge

The human RPE cell line ARPE-19 was purchased from the American Type Culture Collection (ATCC, Rockville, MD, USA). Cells were grown in Dulbecco’s modified eagle

medium (DMEM) (low glucose at 1 g/L or 5.5 mM, Invitrogen, Carlsbad, CA, USA) supplemented with 10 % fetal bovine serum (Atlanta Biologicals, Lawrenceville, GA, USA), 50 μg/ml gentamicin, 0.05 unit/ml penicillin, 50 μg/ml streptomycin (Invitrogen, Carlsbad, CA, USA) at 37 °C in an atmosphere of 95 % air and 5 % CO_2. Cells at passages 8 to14 were used for experiments.

APRE-19 cells were exposed to 36 mM glucose for 48 hours to mimic hyperglycemia in vitro. Such high glucose could maximize significant cellular hyperglycemic response. Mannitol was used as an osmotic control (addition of 30.5 mM mannitol into DMEM low glucose medium to achieve 36 mM).

Knockdown of endogenous AMPKα

Endogenous AMPKα was knocked down by siRNA targeting to AMPKα DNA sequence 5′-GCA TAT GCT GCA GGT AGA TAA -3′. The AMPKα siRNA was transfected into cells using HiPerFect siRNA transfection reagent according to the instructions provided (Qiagen, Valencia, CA, USA). The cells were left for 6 hours to knockdown AMPKα prior to experimentation. Knockdown of AMPKα was monitored by Western blot. The vehicle (transfection reagent) and negative control siRNA (AllStars Negative Control siRNA, Qiagen Inc catalog # 1027281, Valencia, CA, USA) were used as negative controls.

Detection of cellular reactive oxygen species (ROS)

Cellular ROS level was detected by a fluorimetric assay using carboxy-H2DCFDA (C400) as the probe (Invitrogen, Carlsbad, CA, USA). One hundred μL of 4×10^4 cells/mL ARPE-19 cells were seeded into a black 96-well cell culture plate and incubated at 37 °C for 12 hours in a 5 % CO_2 humidified incubator. Following the incubation, cells were treated with high glucose (36 mM) only and/or high glucose with zeaxanthin and/or lutein (at 0.625 and 1.25 μM) for 48 hours. Note, zeaxanthin and/or lutein stock solution was prepared at 10 mM in dimethyl sulfoxide (DMSO). In our preliminary experiments we tested antioxidant effect of DMSO on ARPE-19 cells, and observed that DMSO under 0.05 % had no impact on oxidative stress linked gene expression, and ROS production (data not shown). Cells were then washed with pre-warmed phosphate-buffered saline (PBS). One hundred μL of carboxy-H2DCFDA at 10 μM in PBS was added in each well and cells were further incubated in the culture incubator for additional 45 min. The fluorescence was quantified using a microplate reader with a fluorescence excitation of 485 nm and emission at 538 nm. Relative fluorescence intensity was normalized to untreated ARPE-19 cells (the PBS group) and graphed.

Profiling wolfberry carotenoids by HPLC

The wolfberry carotenoid was profiled by HPLC by Craft Technologies, Inc, Wilson, NC, USA (http://www.crafttechnologies.com/). Carotenoid content was expressed as μg/g fruits (dried fruits).

Determination of water soluble carbohydrates

Water soluble carbohydrate of wolfberry fruits was determined by the anthrone method (19). Fruits were blended into a powder. The powder was mixed with 4.5 volume of deionized water and boiled for 30 min. The mixture was filtered with 4 layers of cheese cloth. The aqueous phase was harvested and subjected to further centrifugation at 1500 × g for 30 min at 4 °C (Thermo Scientific Sorvall RC-5, Waltham, MA, USA). The supernatants were freeze dried. The freeze dried powder was reconstituted in anthrone solution to achieve the solution at 2 g/L anthrone in 75% H_2SO_4. The mixture was boiled at 100 °C for 15 min.

After the samples were cooled down, the absorbance was read at 578 nm using a spectrophotometer. Glucose was used as a standard.

Measurement of total phenolics

Wolfberry fruits were blended into a powder. The powder was mixed with 10 volume of 95 % ethanol, with stirring for 24 hours at 4 °C. Total phenolics were then extracted by reflux extraction three time, 2 h of each at room temperature. The mixture was filtered, and aqueous phase was harvested and subjected to further evaporation to get rid of ethanol. The remaining mass was freeze dried. The freeze dried powder was reconstituted in PBS to achieve water soluble solution for total phenolic measurement.

The amount of total phenolics was determined according to the Folin-Ciocalteu method (20). Ten μL wolfberry water soluble solution (at 1 mg/mL in deionized water) was mixed with 50 μL Folin-Ciocalteau's reagent and 50 μL Na_2CO_3 solution (20%, w/v), then incubated for 2 h at room temperature. After that the absorbance of samples was measured at 760 nm using a spectrophotometer. Results were expressed as mg quercetin equivalent per gram wolfberry fruits.

Western blot

Alteration of retinal protein expression and phosphorylation was determined by Western blot as described (21). Whole retina was dissected under a dissecting microscope. Whole retinal cell lysates and ARPE-19 cell lysates were achieved as described previously (21,22). The primary and secondary antibodies were purchased from Cell Signaling Tech (Danvers, MA). Immunoreactive bands were detected by chemiluminescence (ECL; Thermo Scientific Pierce, Rockford, IL, USA) and visualized by the FluorChem 8800 advanced image system (Alpha Innotech, San Leandro, CA, USA). β-actin was used as a equal loading control. Total pixel intensity of each protein band was normalized to β-actin, and was then used for graphing and statistic analysis.

Light Microscopy

Mouse retinal microscopy was performed as previously described (22). Eye balls were collected and then fixed in a fixative containing 2% paraformaldehyde, 2.5% glutaraldehyde (Sigma-Aldrich, St Louis, MO, USA), and 0.1M cacodylate, then post-fixed with osmium tetroxide (Electron Microscopy Sciences, Fort Washington, PA, USA). Dehydration was in 70% ethanol for 12 h, overnight with 100% ethanol, and 12 h with 100% acetone and finally embedding in Epon LX112 (Electron Microscopy Sciences). Sections were taken perpendicular to the optic nerve so that all of the layers of the retina could be observed. Eyes were sectioned until the optic nerve was observed, so that the depth was consistent in all of the sections. Thick sections (1 μm) were obtained and stained with 1% (W/V) toluidine blue O (Electron Microscopy Sciences) and viewed using a Nikon Eclipse E600 light microscope (Nikon Inc, Melville, NY, USA). The thickness of central retina, the ganglion cell layer (GCL), the inner plexiform layer (IPL), the inner nuclear layer (INL), the outer plexiform layer (OPL), the outer nuclear layer (ONL), and the photoreceptor layer (including the outer segment (OS) and the inner segment (IS)) were measured at the site of 300 μm away from the center of the optic nerves, and analyzed using analySIS software (Soft Imaging System GmbH, Munster, Germany).The ganglion cell number per 100 μm of the ganglion cell layer was counted in the central retinal regions (between 300 and 400 μm away from the center of the optic nerves) (23,24). Structural alteration was analyzed and photographed in the same area of the central retina (around 300 μm away from the center of the optic nerves).

Statistics analysis

All results were expressed as mean ± S.D.. *n* represents the number of mice in each experimental group. Differences in measured variables corresponding to dietary treatment (control and wolfberry) and genotype (wild type and db/db mice) were tested using two-way ANOVA. Data normality was tested using the D'Agostino-Pearson omnibus test. Some data were also tested by the Q-test. The ARPE-19 cell culture experiments were triplicate. The results were analyzed by one-way ANOVA with Dunnett's multiple comparison using SAS 9.1. Representative images of Western blot and light microscopy on retinal structure were shown. The level of significance was considered at $p \leq 0.05$.

Results

Wolfberry is enriched in zeaxanthin, water soluble carbohydrate, and phenolics

Carotenoid HPLC analysis results showed that wolfberry fruits contained significant amount of zeaxanthin (at 1761.3 μg/g fruits), lutein (at 50.9 μg/g fruits), and β-cryptoxanthin (at 25.8 μg/g fruits) (Table 2). Analytical results showed that wolfberry fruits used in this study contained water soluble carbohydrates at 25.2 ± 1.5 % (w/w), and phenolics at 7.8 ± 0.4 mg quercetin equivalent /g fruits.

Wolfberry doesn't lower blood glucose and insulin in db/db type 2 diabetic mice

db/db type 2 diabetic and the genetic background WT mice were fed with control diet (CD) and/or control diet with addition of 1 % (kCal) wolfberry (WD) for 8 weeks, starting at 6 weeks of age. The diet formulas were shown in Table 1. The results demonstrated that db/db mice consumed larger amount of diets than that of WT mice, however, daily food consumption rates of db/db mice were not different within CD and WD diets (Figure 1A). WT mice had greater heart:body weight and kidney:body weight, but lower liver:body weight than those of db/db mice ($p<0.01$, n=21) (Table 3). Supplementation of the wolfberry at 1 % (kCal) did not cause significant difference in the heart, liver, kidney and overall body weight of either db/db or WT mice (Table 3 and Figure 1B).

Fasting blood glucose and plasma insulin were further determined in those animals. As shown in Figure 1C, WT mice had regular fasting blood glucose levels that did not differ by diet. Fasting blood glucose levels were elevated in db/db mice fed CD starting at 6 weeks of age, indicating the development of hyperglycemia. Addition of wolfberry did not lower fasting blood glucose level (WD vs CD). Plasma insulin was measured at study termination (for 8 weeks) (Table 3). The result showed that db/db mice at 14 weeks of age had significant higher insulin levels than that of WT mice ($p<0.05$). No difference was observed by diet (CD vs WD), suggesting that wolfberry at 1 % (kCal) did not systemically improve hyperglycemia and insulin resistance in db/db type 2 diabetic mice.

Wolfberry ameliorates retinal abnormality in db/db type 2 diabetic mice

Retinal thickness and structural alteration were determined by light microscopy. We defined that the central retina thickness is the distance from the ganglion cell layer to the retinal pigment epithelium layer in the central area of retina which is located at around 300 μm away from the center of optic nerves. As shown in Figure 2A, the whole central retina in db/db type 2 diabetic mice was significantly thinner than that of WT mice ($p<0.05$, n=21). Application of dietary wolfberry significantly improved retina thickness in db/db mice (CD vs WD, $p<0.05$). Overall whole retina thickness was not altered in WT mice with or without wolfberry treatment.

Additionally, we measured the thickness of GCL, IPL, INL, OPL, ONL, and photoreceptor layer (IS+OS) and found that the INL and photoreceptor layer (IS+OS) were significant

thinner in db/db mice at 14 weeks of age than that of WT mice ($p<0.05$). However, no significant change was observed in the thickness of the GCL, IPL, OPL, and ONL. Wolfberry improved thickness of the photoreceptor layer and INL in db/db mice (Figure 2A, data on OPL and GCL were not shown).

Ganglion cell number was measured in the central retinal region (Figure 2B). There were significant fewer ganglion cells in diabetic db/db mice fed CD than that of WT mice. Application of wolfberry completely improved the loss of ganglion cells in db/db mice. Ganglion cell number was constant in WT mice with or without wolfberry treatment.

We further investigated retinal structural change in mice with or without wolfberry treatment. As shown in Figure 2C, nuclear distribution in the outer nuclear layer (ONL) was much disorganized in db/db mice fed CD (n=21), compared to WT mice, though overall thickness of ONL was not significantly changed (Figure 2A). We consistently observed a channel-like structure (arrowed in the inserted mage) in the RPE layers of all 21 db/db mice fed CD. No such structure was found in either db/db fed WD, or WT fed CD or WD. Thus we excluded any artifact of the eye tissue processing. This structure might be a very early sign of the disruption of integrity of the RPE layer, though no similar structure has been reported in human diabetic retinopathy. Improvement of those retinal abnormalities was apparently observed in db/db mice fed dietary wolfberry (Figure 2C, the far right panel). Wolfberry caused no structural alteration in WT mice.

Wolfberry attenuates endoplasmic reticulum stress in retina of db/db type 2 diabetic mice

Next we determined the mechanism of wolfberry on restoration of retinal structure in db/db mice. After dietary wolfberry treatment for 8 weeks, the retinal cell lysates of WT and db/db mice were analyzed by Western blot to monitor alteration of ER stress protein expression. Results in Figure 3 A-E demonstrated that elevated protein expression of ER stress biomarkers, BiP, PERK, ATF6, and active caspase-12 occurred in db/db mice fed the control diet, compare to those of WT mice fed the control diet, indicating that db/db mice developed retinal ER stress at 14 weeks of age. Addition of 1 kCal % dietary wolfberry significantly mitigated retinal ER stress as demonstrated by lowered expression of ER stress biomarkers in db/db mice, and in some cases the levels did not differ by diet (CD vs WD) in WT mice ($p<0.05$) (Figure 3 A-E). Caspase-3 activation in retina of db/db mice was significantly inhibited by wolfberry ($p<0.05$) (Figure 3 A, F).

Wolfberry induces protein expression of AMPK, FOXO3α, and antioxidant enzymes thioredoxin and Mn SOD in retina of db/db type 2 diabetic mice

As shown in Figure 4 A-C, AMPKα and phospho-AMPKα Thr172 proteins were significantly down-regulated in retina of db/db mice fed CD, which was normalized by feeding WD ($p<0.05$). Phospho-AMPKα Thr172, but not total AMPKα proteins, was elevated significantly in the wolfberry treated retina of WT mice. The results suggested that addition of wolfberry restored AMPK activity in diabetic retina.

Thioredoxin and Mn SOD are major antioxidant enzymes in scavenging cellular reactive oxygen species (ROS) in the cytoplasma and mitochondria, respectively (25-27). As shown in Figure 4 A, D, and E, the protein expression of thioredoxin and Mn SOD were inhibited in retina of db/db mice fed CD ($p<0.05$). Wolfberry treatment in db/db mice caused elevated expression of thioredoxin and Mn SOD which were comparable to WT mice.

Forkhead O transcription factor 3α (FOXO3α) dually functions as a pro-apoptotic and/or anti-apoptotic transcription factor in response to stress (28,29). Activation of FOXO3α protects cells from oxidative stress in diabetes (30,31). The results in Figure 4 A, F, and G demonstrated that protein levels of phospho-FOXO3α Ser253 and total FOXO3α decreased

significantly in retina of db/db diabetic mice fed CD, which were restored by wolfberry ($p<0.05$). Wolfberry did not alter FOXO3α expression and phosphorylation on Ser253 in the retina of WT mice.

Activation of AMPKα by zeaxanthin and/or lutein protects human RPE cell culture against a high glucose challenge

Finally we wished to determine what potential bioactive constituents of wolfberry exert the influence on retinal protection in db/db mice. Zeaxanthin and lutein which are abundant in wolfberry, has been documented to be specifically transported and accumulated in the RPE and other retinal layers, and acts as a potential antioxidant in prevention of macular degeneration (32,33). Here we used a human adult diploid RPE cell line ARPE-19, to determine their protective effects on a high glucose challenge. In the preliminary study we investigated the glucose dose response in APRE-19 cells and found that exposure to 36 mM glucose could achieve significant hyperglycemic effects in cells, which was similar to human diabetic retina, for instance production of reactive oxygen species, activation of ER stress and apoptosis. Thus, in this report we used 36 mM glucose to mimic hyperglycemia condition in vitro. Mannitol was used as an osmotic control. Zeaxanthin and/or lutein were simultaneously added into the culture medium for 48 hours. Then whole cell lysates were subjected to Western blot. Data showed that the expression levels of proteins (e.g. phospho-AMPKα Thr172, AMPKα, FOXO3α, thioredoxin, Mn SOD) in high glucose challenged cells were significant lower than those in PBS and/or mannitol groups. PERK protein levels were significantly elevated in the cells exposed to high glucose (Figure 5A, $p<0.05$, $n=3$). Both zeaxanthin and/or lutein could mimic wolfberry preventive effect on activation of AMPKα, FOXO3α, Mn SOD, thioredoxin, and inhibition of PERK (Figure 5A, $p<0.05$, $n=3$, only AMPK and PERK mean data shown in lower graphs). Further, we determined that high glucose induced generation of cellular reactive oxygen species (ROS) in ARPE-19 cells. Zeaxanthin and/or lutein mitigated ROS generation dose dependently in ARPE-19 cells exposed to a high glucose challenge (Figure 5B, $p<0.05$, $n=3$, grey columns).

To confirm that AMPKα activation is essential to diminished cellular ROS generation by a high glucose challenge, we knocked down AMPKα by siRNA in the zeaxanthin (1.25 μM) treated ARPE-19 cells under a high glucose challenge (36 mM glucose). Vehicle only (HiPerfect transfection reagent) and the negative control siRNA were used as negative controls. Results clearly demonstrated that knockdown of AMPKα significantly abolished the zeaxanthin effect on normalization of cellular ROS level induced by high glucose ($p<0.05$) (Figure 5 B, far right three black columns: AMPKα siRNA vs Vehicle or Negative siRNA; Figure 6 A and B). Western blot results further showed that knockdown of AMPKα caused significant decreases in protein expression of POXO3α, Mn SOD, thioredoxin, but increases in PERK in high glucose challenged ARPE-19 cells treated with zeaxanthin at 1.25 μM ($p<0.05$) (Figure 6 A and B, each protein expression was normalized to β-actin). Data suggested that AMPKα modulated downstream activities of FOXO3α, thioredoxin and Mn SOD. Zeaxanthin diminished high glucose-induced cellular ROS production and/or ER stress via restoration of AMPKα.

Discussion

In the current study, we investigated the preventive effects of wolfberry on hyperglycemia-induced retinal damage by application of dietary wolfberry at 1 % (kCal) to the db/db mouse, starting at 6 weeks of age while the fasting blood glucose level had been elevated to 189.4± 31.9 mg/dL. The results have demonstrated for the first time that RPE integrity and retinal structure were altered at the early stage of diabetes in the db/db mouse model, and this abnormality could be ameliorated by dietary wolfberry.

The genetically programmed diabetic db/db mouse is an adequate model for studies on the pathogenesis of retinopathy, no retinal disorder occurs in the new born mouse (34). It has been reported that the db/db mouse starts to develop hyperglycemia at 8 weeks of age (35), which was very similar to our observation. Breakdown of blood retinal barrier and leakage of retinal microvessels occurs at 18 weeks of age. About 7 weeks later, severe microvessel leakage and retinopathy are observed (36-40). In the current study we observed that fasting blood glucose level was elevated to >300 mg/dL at 10 weeks of age in db/db fed CD but not WT mice, indicating that the db/db mouse developed hyperglycemia and/or hyperinsulinemia (Figure 1 C) at the similar age as previously reported (34,35). According to publications retinal blood microvessels may still be intact, no blood leakage occurs at this early stage of diabetes in db/db mice (36-40). Thus, the young db/db mouse (<18 weeks of age) would be an excellent type 2 diabetic model for the study in prevention of the development of diabetic retinopathy.

Hyperglycemia induces biochemical abnormality in diabetic cells and tissues, which leads to retinal degeneration. Diabetic retinal degeneration is associated with ganglion cell loss, and reduction of retinal thickness including INL, IPL, and/or ONL (23,41-43). The db/db leptin receptor deficient mouse is a spontaneous type 2 diabetic mouse model. Our finding in loss of ganglion cells was consistent with the previous report (41). We also found for the first time that INL and photoreceptor layers were abnormal compared to WT mice (C57BLKS/J).

Wolfberry fruits have been most popularly consumed as a part of Chinese cuisine though it is also considered as an herbal medicine. Wolfberries are being sold as herbal supplements in Western countries as well (14). Consumption of wolfberries is beneficial to general health, including vision (14-18). In this study we applied a low dose (1 % (kCal)) wolfberry to both WT and db/db mice to mimic what humans would eat on a practical basis. Apparently both types of animals fed the wolfberry supplemented diets survived as well as those fed the control diet as shown in gain of body mass and overall organ weight, suggestive of no obvious side effects at the dose range. However, wolfberry at 1 % (kCal) did not systematically affect the levels of fasting blood glucose and insulin in the diabetic mouse at 14 weeks of age. This may be due to the retinal specific accumulation of its bioactive components zeaxanthin and lutein in mice as discussed below.

The bioactive constituents of wolfberry have been well characterized. The major groups of substance in the wolfberry are carotenoids, polysaccharides, and flavonoids (14). Zeaxanthin and lutein dipalmitates are the most dominant and unique constituents of wolfberry carotenoid fractions (14,15). Zeaxanthin and lutein are specifically transported to and preferentially taken up, and accumulated in retinal cells by sharing the transportation pathway of HDL cholesterol (32,33). It has been suggested that in the retina zeaxanthin and/or lutein bind to antioxidant enzymes which in turn stabilize the proteins under chronic oxidative stress in the case of macular degeneration (32, 40-46). Recently Gierhart and colleagues reported that zeaxanthin administration at 0.02 % or 0.1 % (diet by weight) significantly inhibited diabetes-induced retinal oxidative damage, but no effect was achieved on the severity of hyperglycemia in rats at the early stage of diabetes (47). In the current study we used wolfberry fruits and pure zeaxanthin and/or lutein to treat diabetic mice and human RPE cells, respectively. The results suggested that wolfberry protected retinal cells against a high glucose challenge locally but not systemically, at least partially, if not all, through zeaxanthin and/or lutein, though there may be some potential synergistic interactions of other bioactive components in wolfberry, such as phenolics and polysaccharides.

AMPK is a cellular energy sensor in mammals. It is down-regulated in type 2 diabetic patients (3-5). Targeting AMPK has been suggested as a most successful pharmaceutical

strategy for type 2 diabetes. For instance, metformin, an oral anti-diabetic drug, at least partially works through activation of AMPK (6,48). Wolfberry induced AMPK activation in wild type mice, increased AMPK at protein level in db/db mice (Figure 4 A, B, C). Retinal AMPK activation may be due to retinal specific accumulation of zeaxanthin and/or lutein. Further, wolfberry restored FOXO3α (Figure 4 F and G). Data suggested that wolfberry protection of retina from caspase-3 dependent apoptosis may be through regulation of protein expression, centered by AMPK activation.

FOXO3α is regulated by AKT/PKB, extracellular signal-regulated kinases, and AMPK. It is essential to cell survival in diabetes (31,49,50). FOXO3α is being clinically shown to achieve the therapeutic effects (30,31). Down-regulation of FOXO3α results in disruption of cellular ubiquitination and inhibition of antioxidant activity. AMPK up-regulation of FOXO3α has been suggested to account for increased expression of antioxidant enzymes thioredoxin and Mn SOD in diabetic endothelial cells (50). Application of wolfberry caused up-regulation of retinal FOXO3α and thioredoxin and Mn SOD (Figure 4), which may lead to diminishing cellular ROS generation. Increased thioredoxin and Mn SOD by dietary wolfberry may be due to up-regulation of gene expression and/or stabilization of existing proteins by zeaxanthin and/or lutein under hyperglycemia. The cell culture study further suggested that wolfberry restoration of thioredoxin and Mn SOD would help rebalance cellular redox homeostasis through normalization of cellular ROS status.

ER stress has been exclusively documented to be a major driven force to cellular oxidative retinal damage at the late stage of diabetes (10,51). We have demonstrated in this study that hyperglycemia induced elevated protein expression of ER stress biomarkers in early diabetic retina in vivo, indicating that hyperglycemia accounts for retinal endoplasmic reticulum (ER) stress, inhibition of AMPKα, thioredoxin, Mn SOD, FOXO3α, and retinal abnormality. This was further confirmed by in vitro studies on human retinal ARPE-19 cells when they were exposed to a high glucose challenge (Figure 5A). This was not due to osmotic pressure as mannitol alone did not differ from phosphate buffered saline (PBS) controls. Prolonged hyperglycemia (or high glucose) distinctly induces generation of cellular ROS (Figure 5B), which was diminished by administration of whole wolfberries and/or the bioactive fractions zeaxanthin and lutein. AMPKα siRNA knockdown results further suggested that zeaxanthin diminished high glucose-induced cellular ROS levels via restoration of AMPKα. AMPKα is the upstream modulator of FOXO3α and thioredoxin and Mn SOD.

Taken together, dietary wolfberry and/or its bioactive constituents zeaxanthin and lutein functioned as modulators of cell survival/death signaling pathways, through targeting pathways in AMPK and FOXO3α signaling, resulting in normalization of cellular ROS and subsequent attenuation of ER stress. This could lead to prevention of retinal apoptosis and restoration of retinal structure in the type 2 diabetic mouse (Figure 7). Dietary treatments using individual fractions isolated from the wolfberry would be necessary for further mechanistic studies in vivo. To our knowledge, this is the first report that wolfberry bioactive constituents prevented or delay the onset of the disease of diabetic retinopathy in an animal mode.

Acknowledgments

The authors would like to express their gratitude to the staff of KSU Animal Resource Facility for animal care.

LT, YZ, YJ, LW, EO, LW conducted research; DM, DL, designed research; LT, YZ, YJ, LW, DM, DL, analyzed data; DM, DL, wrote the manuscript; D. L., had primary responsibility for final content. All authors read and approved the final manuscript. LT, YZ, YJ, contributed equally to this study.

Financial support: the Kansas State University (KSU) NIH NCRR Grant P20-RR-017686 (to D.L.). Contribution no. 11-177-J from the Kansas Agricultural Experiment Station.

Abbreviation

AMPK	AMP-activated protein kinase
ATF6	activating transcription factor 6
BiP	binding immunoglobulin protein
db/db	leptin receptor deficient mouse
ER	endoplasmic reticulum
FOXO3α	forkhead O transcription factor 3 α
IRE1	inositol-requiring protein 1
IS	inner segment
CD	control diet
WD	control diet with 1 % (kCal) wolfberry
OS	outer segment
PERK	protein kinase RNA-like ER kinase
ROS	reactive oxygen species
RPE	retinal pigment epithelium
siRNA	small interfering RNA
SOD	superoxide dismutase
WT	wild type mouse

References

1. Busik JV, Mohr S, Grant MB. Hyperglycemia-induced reactive oxygen species toxicity to endothelial cells is dependent on paracrine mediators. Diabetes. 2008; 57:1952–1965. [PubMed: 18420487]
2. Nathan, David M.; Buse, John B.; Davidson, Mayer B.; Heine, Robert J.; Holman, Rury R.; Sherwin, Robert; Zinman, Bernard. Management of hyperglycemia in type 2 diabetes: A consensus algorithm for the initiation and adjustment of therapy: A consensus statement from the American Diabetes Association and the European Association for the Study of Diabetes. Diabetes Care. 2006; 29:1963–1972. [PubMed: 16873813]
3. Sanz P. AMP-activated protein kinase: structure and regulation. Curr Protein Pept Sci. 2008; 9:478–492. [PubMed: 18855699]
4. Zhang BB, Zhou G, Li C. AMPK: an emerging drug target for diabetes and the metabolic syndrome. Cell Metab. 2009; 9:407–416. [PubMed: 19416711]
5. Kukidome D, Nishikawa T, Sonoda K, Imoto K, Fujisawa K, Yano M, Motoshima H, Taguchi T, Matsumura T, Araki E. Activation of AMP-activated protein kinase reduces hyperglycemia-induced mitochondrial reactive oxygen species production and promotes mitochondrial biogenesis in human umbilical vein endothelial cells. Diabetes. 2006; 55:120–127. [PubMed: 16380484]
6. Leverve XM, Guigas B, Detaille D, Batandier C, Koceir EA, Chauvin C, Fontaine E, Wiernsperger NF. Mitochondrial metabolism and type-2 diabetes: a specific target of metformin. Diabetes Metab. 2003; 29:S88–94.
7. Rutter GA, Leclerc I. The AMP-regulated kinase family: enigmatic targets for diabetes therapy. Mol Cell Endocrinol. 2009; 297:41–49. [PubMed: 18611432]
8. Kim I, Xu W, Reed JC. Cell death and endoplasmic reticulum stress: disease relevance and therapeutic opportunities. Nat Rev Drug Discov. 2008; 7:1013–1030. [PubMed: 19043451]
9. Malhotra JD, Kaufman RJ. Endoplasmic reticulum stress and oxidative stress: a vicious cycle or a double-edged sword? Antioxid Redox Signal. 2007; 9:2277–2293. [PubMed: 17979528]

10. Oshitari T, Hata N, Yamamoto S. Endoplasmic reticulum stress and diabetic retinopathy. Vasc Health Risk Manag. 2008; 4:115–122. [PubMed: 18629365]
11. Potterat O. Goji (Lycium barbarum and L. chinense): Phytochemistry, pharmacology and safety in the perspective of traditional uses and recent popularity. Planta Med. 2010; 76:7–19. [PubMed: 19844860]
12. Ron D, Walter P. Signal integration in the endoplasmic reticulum unfolded protein response. Nat Rev Mol Cell Biol. 2007; 8:519–529. [PubMed: 17565364]
13. Görlach A, Klappa P, Kietzmann T. The endoplasmic reticulum: folding, calcium homeostasis, signaling, and redox control. Antioxid Redox Signal. 2006; 8:1391–1418. [PubMed: 16986999]
14. Faitova J, Krekac D, Hrstka R, Vojtesek B. Endoplasmic reticulum stress and apoptosis. Cell Mol Biol Lett. 2006; 11:488–505. [PubMed: 16977377]
15. Inbaraj BS, Lu H, Hung CF, Wu WB, Lin CL, Chen BH. Determination of carotenoids and their esters in fruits of Lycium barbarum Linnaeus by HPLC-DAD-APCI-MS. J Pharm Biomed Anal. 2008; 47:812–818. [PubMed: 18486400]
16. Inbaraj BS, Lu H, Kao TH, Chen BH. Simultaneous determination of phenolic acids and flavonoids in Lycium barbarum Linnaeus by HPLC-DAD-ESI-MS. J Pharm Biomed Anal. 2010; 51:549–556. [PubMed: 19819093]
17. Chang RC, So KF. Use of anti-aging herbal medicine, Lycium barbarum, against aging-associated diseases. What do we know so far? Cell Mol Neurobiol. 2008; 28:643–652. [PubMed: 17710531]
18. Ho YS, So KF, Chang RC. Anti-aging herbal medicine--how and why can they be used in aging-associated neurodegenerative diseases? Ageing Res Rev. 2010; 9:354–362. [PubMed: 19833234]
19. Yemm EW, Willis AJ. The estimation of carbohydrates in plant extracts by anthrone. Biochem J. 1954; 57:508–514. [PubMed: 13181867]
20. Peri C, Pompei C. An assay of different phenolic fractions in wines. Am J Enol Vitic. 1971; 22:55–58.
21. Lin D, Takemoto DJ. Oxidative activation of protein kinase Cgamma through the C1 domain. Effects on gap junctions. J Biol Chem. 2005; 280:13682–13693. [PubMed: 15642736]
22. Yevseyenkov VV, Das S, Lin D, Willard L, Davidson H, Sitaramayya A, Giblin FJ, Dang L, Takemoto DJ. Loss of protein kinase Cgamma in knockout mice and increased retinal sensitivity to hyperbaric oxygen. Arch Ophthalmol. 2009; 127:500–506. [PubMed: 19365031]
23. Arnal E, Miranda M, Johnsen-Soriano S, Alvarez-Nölting R, Díaz-Llopis M, Araiz J, Cervera E, Bosch-Morell F, Romero FJ. Beneficial effect of docosahexanoic acid and lutein on retinal structural, metabolic, and functional abnormalities in diabetic rats. Curr Eye Res. 2009; 34:928–938. [PubMed: 19958109]
24. Béby F, Housset M, Fossat N, Le Greneur C, Flamant F, Godement P, Lamonerie T. Otx2 gene deletion in adult mouse retina induces rapid RPE dystrophy and slow photoreceptor degeneration. PLoS One. 2010; 5:e11673. [PubMed: 20657788]
25. Jones DP. Redox sensing: orthogonal control in cell cycle and apoptosis signalling. J Intern Med. 2010; 268:432–448. [PubMed: 20964735]
26. Nishikawa T, Araki E. Impact of mitochondrial ROS production in the pathogenesis of diabetes mellitus and its complications. Antioxid Redox Signal. 2007; 9:343–353. [PubMed: 17184177]
27. Kim A, Joseph S, Khan A, Epstein CJ, Sobel R, Huang TT. Enhanced expression of mitochondrial superoxide dismutase leads to prolonged in vivo cell cycle progression and up-regulation of mitochondrial thioredoxin. Free Radic Biol Med. 2010; 48:1501–1512. [PubMed: 20188820]
28. Tremblay ML, Giguère V. Phosphatases at the heart of FoxO metabolic control. Cell Metab. 2008; 7:101–103. [PubMed: 18249169]
29. Maiese K, Chong ZZ, Hou J, Shang YC. The “O” class: crafting clinical care with FoxO transcription factors. Adv Exp Med Biol. 2009; 665:242–260. [PubMed: 20429429]
30. Kops GJ, Dansen TB, Polderman PE, Saarloos I, Wirtz KW, Coffer PJ, Huang TT, Bos JL, Medema RH, Burgering BM. Forkhead transcription factor FOXO3a protects quiescent cells from oxidative stress. Nature. 2002; 419:316–321. [PubMed: 12239572]
31. Li XN, Song J, Zhang L, LeMaire SA, Hou X, Zhang C, Coselli JS, Chen L, Wang XL, Zhang Y, Shen YH. Activation of the AMPK-FOXO3 pathway reduces fatty acid-induced increase in

intracellular reactive oxygen species by upregulating thioredoxin. Diabetes. 2009; 58:2246–2257. [PubMed: 19592618]

32. Li B, Vachali P, Bernstein PS. Human ocular carotenoid-binding proteins. Photochem Photobiol Sci. 2010; 9:1418–1425. [PubMed: 20820671]
33. During A, Doraiswamy S, Harrison EH. Xanthophylls are preferentially taken up compared with beta-carotene by retinal cells via a SRBI-dependent mechanism. J Lipid Res. 2008; 49:1715–1724. [PubMed: 18424859]
34. Midena E, Segato T, Radin S, di Giorgio G, Meneghini F, Piermarocchi S, Belloni AS. Studies on the retina of the diabetic db/db mouse. I. Endothelial cell-pericyte ratio. Ophthalmic Res. 1989; 21:106–111. [PubMed: 2734001]
35. Tadayoni R, Paques M, Gaudric A, Vicaut E. Erythrocyte and leukocyte dynamics in the retinal capillaries of diabetic mice. Exp Eye Res. 2003; 77:497–504. [PubMed: 12957148]
36. Clements RS Jr, Robison WG Jr, Cohen MP. Anti-glycated albumin therapy ameliorates early retinal microvascular pathology in db/db mice. J Diabetes Complications. 1998; 12:28–33. [PubMed: 9442812]
37. Barile GR, Pachydaki SI, Tari SR, Lee SE, Donmoyer CM, Ma W, Rong LL, Buciarelli LG, Wendt T, Hörig H, Hudson BI, Qu W, Weinberg AD, Yan SF, Schmidt AM. The RAGE axis in early diabetic retinopathy. Invest Ophthalmol Vis Sci. 2005; 46:2916–2924. [PubMed: 16043866]
38. Cheung AK, Fung MK, Lo AC, Lam TT, So KF, Chung SS, Chung SK. Aldose reductase deficiency prevents diabetes-induced blood-retinal barrier breakdown, apoptosis, and glial reactivation in the retina of db/db mice. Diabetes. 2005; 54:3119–3125. [PubMed: 16249434]
39. Li J, Wang JJ, Chen D, Mott R, Yu Q, Ma JX, Zhang SX. Systemic administration of HMG-CoA reductase inhibitor protects the blood-retinal barrier and ameliorates retinal inflammation in type 2 diabetes. Exp Eye Res. 2009; 89:71–78. [PubMed: 19254713]
40. Li J, Wang JJ, Yu Q, Chen K, Mahadev K, Zhang SX. Inhibition of reactive oxygen species by Lovastatin downregulates vascular endothelial growth factor expression and ameliorates blood-retinal barrier breakdown in db/db mice: role of NADPH oxidase 4. Diabetes. 2010; 59:1528–1538. [PubMed: 20332345]
41. Sohn EJ, Kim YS, Kim CS, Lee YM, Kim JS. KIOM-79 prevents apoptotic cell death and AGEs accumulation in retinas of diabetic db/db mice. J Ethnopharmacol. 2009; 121:171–174. [PubMed: 19013511]
42. Yeung CM, Lo AC, Cheung AK, Chung SS, Wong D, Chung SK. More severe type 2 diabetes-associated ischemic stroke injury is alleviated in aldose reductase-deficient mice. J Neurosci Res. 2010; 88:2026–2034. [PubMed: 20143423]
43. Sasaki M, Ozawa Y, Kurihara T, Kubota S, Yuki K, Noda K, Kobayashi S, Ishida S, Tsubota K. Neurodegenerative influence of oxidative stress in the retina of a murine model of diabetes. Diabetologia. 2010; 53:971–979. [PubMed: 20162412]
44. Bernstein PS, Balashov NA, Tsong ED, Rando RR. Retinal Tubulin binds macular carotenoids. Invest Ophthalmol Vis Sci. 1997; 38:167–175. [PubMed: 9008641]
45. Crabtree DV, Ojima I, Geng X, Adler AJ. Tubulins in the primate retina: evidence that xanthophylls may be endogenous ligands for the paclitaxel-binding site. Bioorg Med Chem. 2001; 9:1967–1976. [PubMed: 11504633]
46. Bhosale, Larson AJ, Frederick J, Southwick K, Thulin CD, Bernstein PS. Identification and characterization of a pi isoform of glutathione S-transferase as a zeaxanthin-binding protein in the macula of the human eye. J Biol Chem. 2004; 279:49447–49454. [PubMed: 15355982]
47. Kowluru RA, Menon B, Gierhart DL. Beneficial effect of zeaxanthin on retinal metabolic abnormalities in diabetic rats. Invest Ophthalmol Vis Sci. 2008; 49:1645–1651. [PubMed: 18385086]
48. Hou X, Song J, Li XN, Zhang L, Wang X, Chen L, Shen YH. Metformin reduces intracellular reactive oxygen species levels by upregulating expression of the antioxidant thioredoxin via the AMPK-FOXO3 pathway. Biochem Biophys Res Commun. 2010; 396:199–205. [PubMed: 20398632]
49. Katoh M, Katoh M. Human FOX gene family (Review). Int J Oncol. 2004; 25:1495–1500. [PubMed: 15492844]

50. Kukidome D, Nishikawa T, Sonoda K, Imoto K, Fujisawa K, Yano M, Motoshima H, Taguchi T, Matsumura T, Araki E. Activation of AMP-activated protein kinase reduces hyperglycemia-induced mitochondrial reactive oxygen species production and promotes mitochondrial biogenesis in human umbilical vein endothelial cells. Diabetes. 2006; 55:120–127. [PubMed: 16380484]

51. Li J, Wang JJ, Yu Q, Wang M, Zhang SX. Endoplasmic reticulum stress is implicated in retinal inflammation and diabetic retinopathy. FEBS Lett. 2009; 583:1521–1527. [PubMed: 19364508]

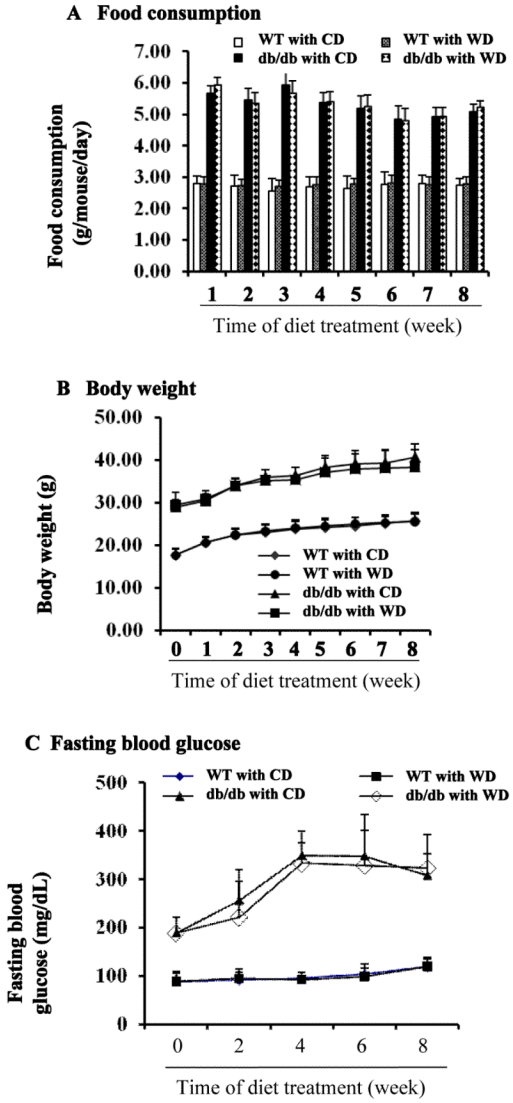

Figure 1. Food consumption, body weight, and fasting blood glucose in wild type (WT) and db/db type 2 diabetic mice

Six-week old male wild type (WT) and db/db diabetic mice (db/db) were fed the control diet (CD) or the control diet with 1 % (kCal) wolfberry (WD) for 8 weeks. Food consumption (**A**) and body weight (**B**) were monitored weekly. Fasting blood glucose (**C**) was tracked biweekly. n=21

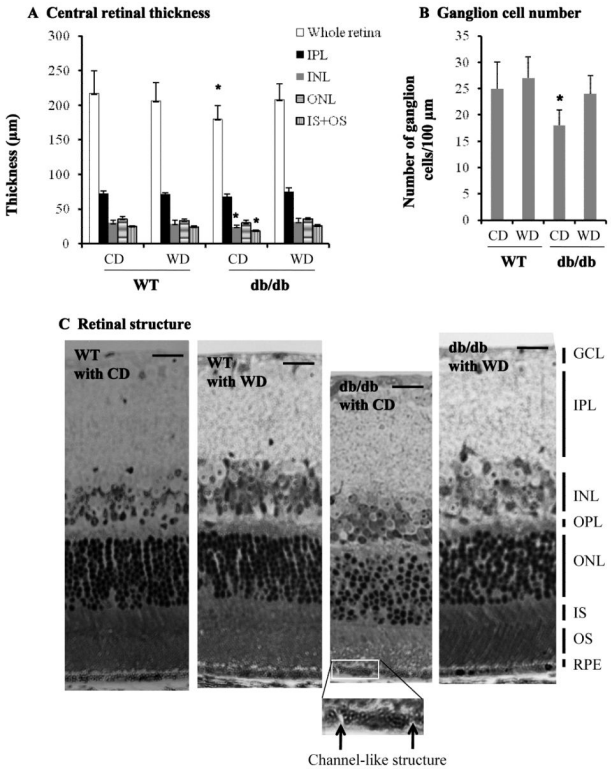

Figure 2. Wolfberry improves retinal abnormality in db/db type 2 diabetic mice

After dietary treatments mouse eye balls were fixed, and thick retina sections were prepared as described in the Materials and Methods section. **A.** The central retinal thickness, and the inner plexiform layer, inner nuclear layer, outer nuclear layer, and photoreceptor layer (IS +OS) were measured and graphed (n=21). * $p < 0.05$ vs. WT with CD. **B.** Ganglion cells were counted and graphed as described in the Methods section. Loss of ganglion cells in the db/db mouse fed CD was significant. * $p < 0.05$ vs. WT with CD. **C.** Retinal structure of WT and db/db mice after dietary treatments. The inserted picture showing a channel-like structure in the retinal pigment epithelial (RPE) cell layer of db/db type 2 diabetic mice (arrowed) (n=21). GCL, the ganglion cell layer; IPL, the inner plexiform layer; INL, the inner nuclear layer; ONL, the outer nuclear layer; IS, the inner segment layer; OS, the outer segment layer; RPE, the retinal pigment epithelium layer. WT, wild type mice; db/db, db/db type 2 diabetic mice; CD, control diet; WD, control diet with 1 % (kCal) wolfberry. Scale bar, 10 μm

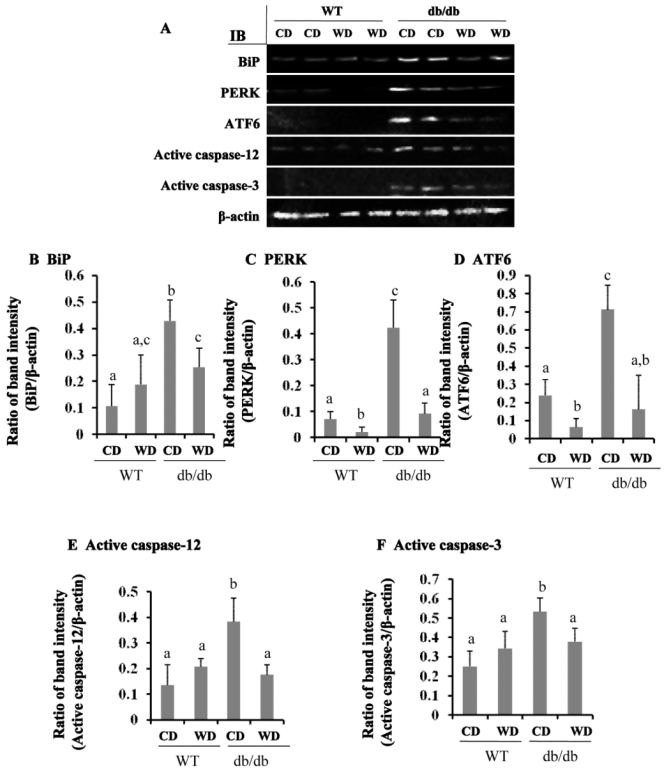

Figure 3. Attenuation of endoplasmic reticulum (ER) stress by dietary wolfberry in db/db type 2 diabetic mice

After dietary treatments, animals were euthanized. The whole retina was isolated and subjected to Western blot. Representative images were shown (A). β-actin was used as an euqal loading control to normalize each protein expression. Relative band intensity of each protein to β-actin was used for graphing and statistic analysis. n=21. In all cases, the statistic significance at $p \leq 0.05$ was marked by different letters a,b, and/or c. CD, control diet; WD, control diet with 1 % (kCal) wolfberry. BiP, binding immunoglobulin protein (also named as glucose regulated protein 78, GRP78); PERK, protein kinase RNA-like ER kinase; ATF6, activating transcription factor -6; IB, immunoblot. **A**. Representative images; **B**, BiP; **C**, PERK; **D**, ATF6; **E**, active caspase-12; **F**, active caspase-3.

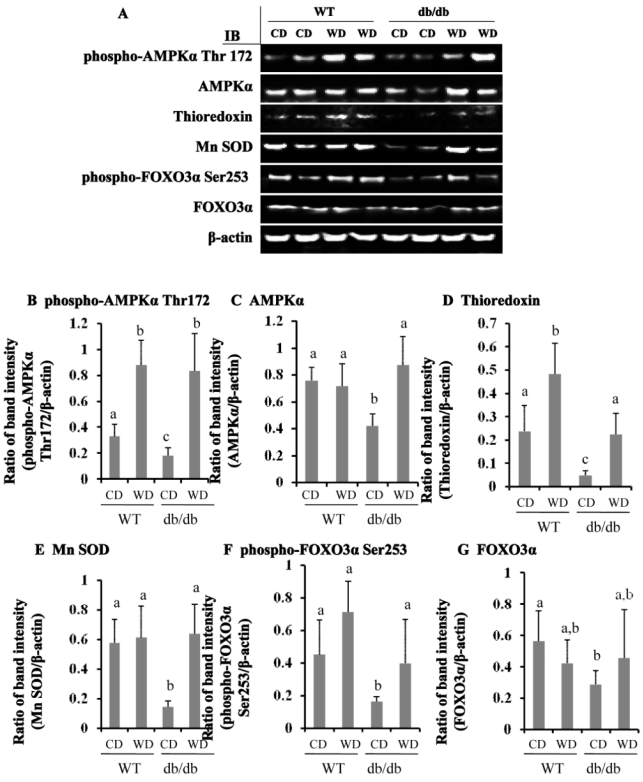

Figure 4. Wolfberry restores AMPK, FOXO3α, and antioxidant enzymes thioredoxin and Mn SOD in retina of db/db type 2 diabetic mice

Whole retina was isolated and subjected to Western blot at study termination. Representative images were shown (**A**). β-actin was used as an equal loading control to normalize each protein expression. Relative band intensity of each protein to β-actin was used for graphing and statistic analysis. n=21. The statistic significance at $p \leq 0.05$ was marked by different letters a,b, and/or c. CD, control diet; WD, control diet with 1 % (kCal) wolfberry. AMPKα, AMP activated protein kinase α; Mn SOD, Mn superoxide dismutase; FOXO3α, Forkhead O transcription factor O 3α. **B**, phospho-AMPKα Thr172; **C**, AMPKα; **D**, thioredoxin; **E**, Mn SOD; **F**, phospho-FOXO3α Ser253; **G**, FOXO3α

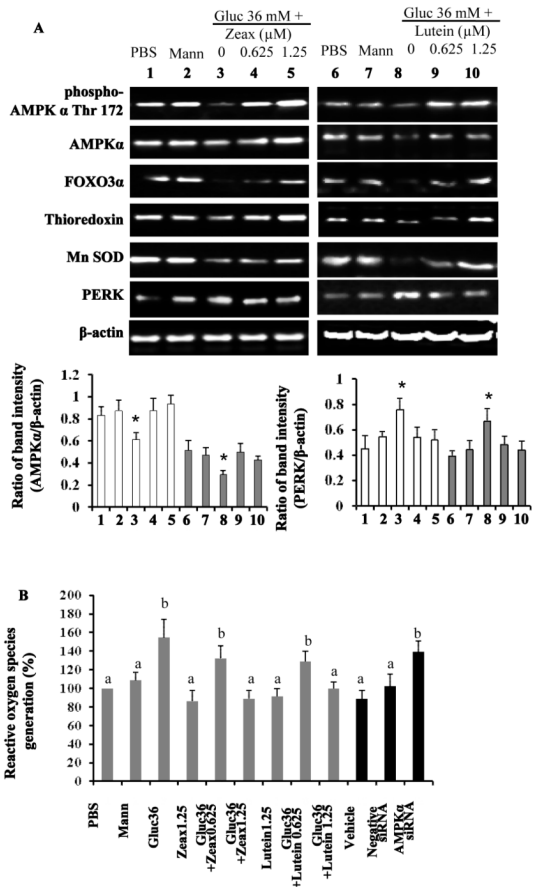

Figure 5. Zeaxanthin and/or lutein activation of AMPK protects human RPE cell culture against a high glucose challenge

Human adult diploid RPE cell line ARPE-19 cells were treated with 36 mM glucose for 48 hours to mimic hyperglycemia condition in db/db mice. Zeaxanthin and/or lutein were simultaneously added into the culture medium. Mannitol was used as an osmotic control. The whole cell lysates were subjected to Western blot (**A**). β-actin was used as an euqal loading control to normalize each protein expression. Relative band intensity of each protein to β-actin was used for graphing and statistic analysis (* $p<0.05$, n=3, mean data on AMPK and PERK shown in lower graphs. Other mean data not shown). Zeaxanthin group samples #1 to #5: PBS, mannitol, glucose only, glucose with zeaxanthin 0.625 μM, and glucose with zeaxanthin 1.25 μM, * $p<0.05$ vs. the PBS (sample #1). Lutein group samples #6 to #10: PBS, mannitol, glucose only, glucose with lutein 0.625 μM, and glucose with lutein 1.25 μM, * $p<0.05$ vs. the PBS (sample #6).. The cellular reactive oxygen species (ROS) level was determined (**B**). AMPKα was knocked down by its specific siRNA in the zeaxanthin (1.25 μM) treated ARPE-19 cells under a high glucose challenge. AMPKα siRNA knockdown-altered cellular ROS level was determined and expressed in the far right three black columns of graph **B** ($p<0.05$ vs the Vehicle). PBS, phosphate buffered saline; Mann, mannitol; Gluc, glucose; Zeax, zeaxanthin

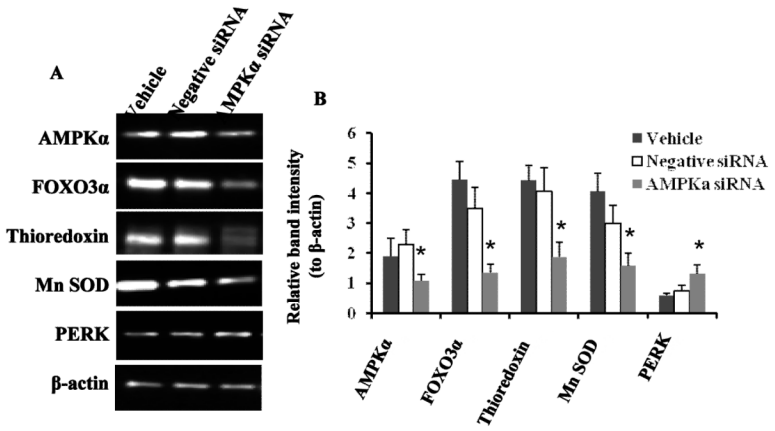

Figure 6. siRNA knockdown of AMPK*α* causes significant decreases in protein expression of POXO3*α*, Mn SOD, thioredoxin, but increases in PERK in high glucose challenged ARPE-19 cells

AMPKα was knocked down by its specific siRNA in the zeaxanthin (1.25 μM) treated ARPE-19 cells under a high glucose challenge. Alteration of protein expression was monitored by Western blot. Representative images were shown (**A**). β-actin was used as an equal loading control to normalize each protein expression. Relative band intensity of each protein to β-actin was used for graphing and statistic analysis (**B**). * $p<0.05$ vs. the Vehicle groups

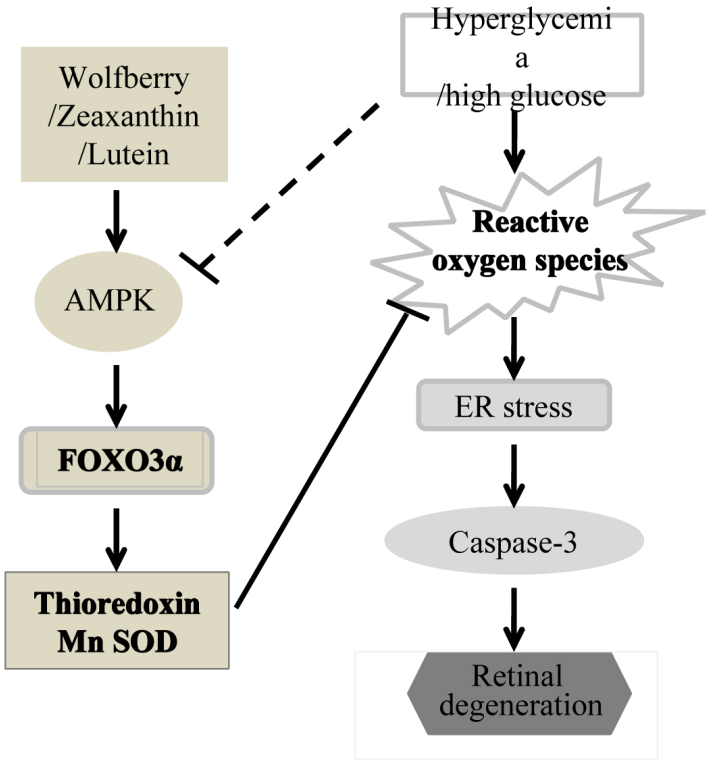

Figure 7. Schematic diagram showing wolfberry and/or zeaxanthin and lutein modulated retinal protection in type 2 diabetes

Dietary wolfberry restores AMPK, at least partially, through zeaxanthin and/or lutein. Restoration of AMPK and FOXO3α signaling leads to enhanced expression of thioredoxin and Mn SOD which in turn results in normalization of cellular ROS and attenuation of ER stress. This could lead to prevention of retinal apoptosis and restoration of retinal structure in the type 2 diabetic mouse. Dash line represents multiple steps.

Table 1

Diet formulas of the control diet (CD, 10 kCal % fat) and wolfberry diet (WD, control diet with 1 % (kCal) wolfberry), formulated by the Research Diets Inc (New Brunswick, NJ, USA)

Diet Ingredient (g)	CD	WD
Casein	200	198.7
L-cystine	3	3
Com starch	315	311.4
Maltodextrin 10	35	35
Sucrose	350	346.4
Cellulose	50	48.9
Soybean oil	25	24.5
Lard	20	19.5
Mineral mix SI0026	10	10
Dicalcium phosphate	13	13
Calcium carbonate	5.5	5.5
Potassium citrate, 1H20	16.5	16.5
Vitamin mix VI0001	10	10
Choline bitartrate	2	2
Wolfberry	**0**	**10.7**
Total	1055	1055.1

Table 2

Wolfberry carotenoid profile by HPLC

Carotenoid	μg/g wolfberry fruits
Zeaxanthin	1761.3
Lutein	50.9
β-cryptoxanthin	25.8
α-cryptoxanthin	<0.1
Lycopene	<0.1
cis-lycopene	<0.1
α-carotene	<0.1
β-carotene	<0.1
cis-β-carotene	<0.1

Table 3

Dietary wolfberry does not alter mouse organ weight and fasting plasma insulin level (mean±S.D., n=21)

Animal	Diet	Kidney/BW (g/g)	Liver/BW (g/g)	Heart/BW (g/g)	Fasting plasma insulin (ng/mL)
WT	CD	0.016 ± 0.0013	0.038 ± 0.0018	0.0061 ± 0.0005	0.71 ± 0.329
	WD	0.017 ± 0.0012	0.039 ± 0.0021	0.0062 ± 0.0004	0.53 ± 0.302
db/db	CD	0.011 ± 0.0009[a]	0.065 ± 0.0035[b]	0.0028 ± 0.0003[c]	3.69 ± 1.094[d]
	WD	0.011 ± 0.0007[a]	0.061 ± 0.0029[b]	0.0031 ± 0.0003[c]	4.42 ± 1.863[d]

BW, body weight; CD, control diet; WD, wolfberry diet; WT, wild type mouse

[a] p<0.01 vs. WT group with CD

[b] p<0.01 vs. WT group with CD

[c] p<0.01 vs. WT group with CD

[d] p<0.05 vs. WT group with CD